Magneto-transport Effects in Topological Insulator Bi_2Se_3 Nanoribbons

Hao Tang, Dong Liang, Richard L.J. Qiu, and Xuan P.A Gao*
Department of Physics, Case Western Reserve University, Cleveland, Ohio 44106

Magneto-resistance (MR) of Bi_2Se_3 nanoribbons is studied over a broad range of temperature (T=300K-2K) and under various magnetic field (B) orientations. The MR is strongly anisotropic with the perpendicular MR much larger than the longitudinal and transverse MRs. The perpendicular MR exhibits quadratic B-dependence in low fields and becomes linear at high B. However, when T increases, the perpendicular MR becomes linear over the whole magnetic field range (0-9T) up to room temperature. This unusual linear MR is discussed in the context of the quantum linear MR of the topological surface-states. We also observe the boundary-scattering effect in MR at low temperatures, which indicates that the out-of-plane Fermi momentum is much smaller the in-plane Fermi momentum, excluding the simple three-dimensional Fermi surface picture.

PACS numbers: 73.20.-r,73.25.+i,73.63.-b,03.65.Vf

Topological insulators are a class of quantum materials that have insulating energy gaps in the bulk, and gapless surface states on the sample boundary that are protected by time-reversal symmetry[1–3]. Recently, Bi_2Se_3 and related materials[4] have been proposed as three-dimensional (3D) topological insulators with a single Dirac cone for the surface states. Among these materials, Bi_2Se_3, which is a pure compound rather than an alloy like Bi_xSb_{1-x}[5], owns a larger gap (0.3 eV), and is thought to be promising for room temperature applications. The existence of a Z2 topological phase with a surface Berry's phase in the stoichiometric compound Bi_2Se_3 has been observed by angle-resolved photoemission spectroscopy[6, 7]. To enhance the contribution of the surface states in transport measurements, Bi_2Se_3 nanowires and nanoribbons offer an attractive alternative to bulk samples for studying the Dirac electrons on surface due to their high surface-to-volume ratio[8, 9]. Indeed, Aharonov-Bohm (AB) oscillations in the longitudinal MR of Bi_2Se_3 nanoribbons were discovered, proving the existence of a coherent surface conducting channel[8]. Here, we study the MR of Bi_2Se_3 nanoribbons under various magnetic field orientations to elucidate the transport mechanism in these novel nanomaterials. Our measurements reveal boundary scattering effects and a linear MR in the perpendicular field configuration that persists to room temperature. This striking linear MR is discussed in the context of quantum linear MR (QLMR) of systems with linear dispersion spectrum [10], consistent with the transport through topological surface-states.

Pure Bi_2Se_3 nanoribbons are synthesized in a horizontal tube furnace via the vapor-liquid-solid mechanism with gold particles as catalysts, similar to literature[8, 9]. Typical Bi_2Se_3 nanoribbons have thickness ranging from 50-400 nm and widths ranging from 200 nm to several μms. Energy dispersive X-ray spectroscopy analyses reveal uniform chemical composition with a Bi/Se atomic ratio about 2:3, indicating the stoichiometric Bi_2Se_3. High-resolution TEM imaging and 2D Fourier transformed electron diffraction measurements demonstrate that the samples are single-crystalline rhombohedral phase and grow along the $[11\overline{2}0]$ direction. The upper and lower surfaces are (0001) planes. The as-grown samples are suspended in ethanol by sonication and dispersed on a heavily doped Si substrate with 300nm SiO_2 on its surface. Photolithography is used to pattern four electrodes contacting single nanoribbon. The electrodes consist of 150nm Pd with a 5nm Ti adhesion layer formed via e-beam evaporation and lift-off. Ohmic contacts are obtained without annealing. The transport measurements are performed in a Quantum Design PPMS with low frequency lockin technique.

Temperature dependent four-terminal resistance R of a nanoribbon (sample #1) from room temperature down to 2K is shown in Fig. 1a. Four-terminal resistance of the nanoribbons is obtained by flowing a current I (typically 0.1-1 μA) through the two outer contacts and monitoring the voltage drop V between the two inner contacts (typical spacing 2μm) as shown in SEM image in Fig.1a inset. The resistance decreases with the temperature, starts to saturate around 25K, and then remains nearly flat down to 2K, the minimum temperature reached during these measurements. This metallic $R(T)$ is typical behavior for heavily doped semiconductors, and can result from the small band gap of Bi_2Se_3 and the residual doping from intrinsic defects such as Se vacancies[11].

The perpendicular (B perpendicular to both current flow and nanoribbon surface) MR of sample #1 is shown in Fig.1b from T=300K down to 2K. First of all, it is striking that there is significant (5-25%) MR for this configuration at temperatures all the way up to 300K, and the MR curves appear to be parallel to each other. Second, the MR has a linear B dependence up to 9T, the highest B achieved in our PPMS, for temperatures higher than 90K. As T decreases below 90K, $R(B)$ takes an approximately quadratic dependence below 3T. This evolution of MR can be seen more clearly in Fig.1c where the normalized resistance $R(B)/R(B=0)$ is plotted against B. It has been known for a long time that for metals with open Fermi surfaces (e.g. Au), the MR could be

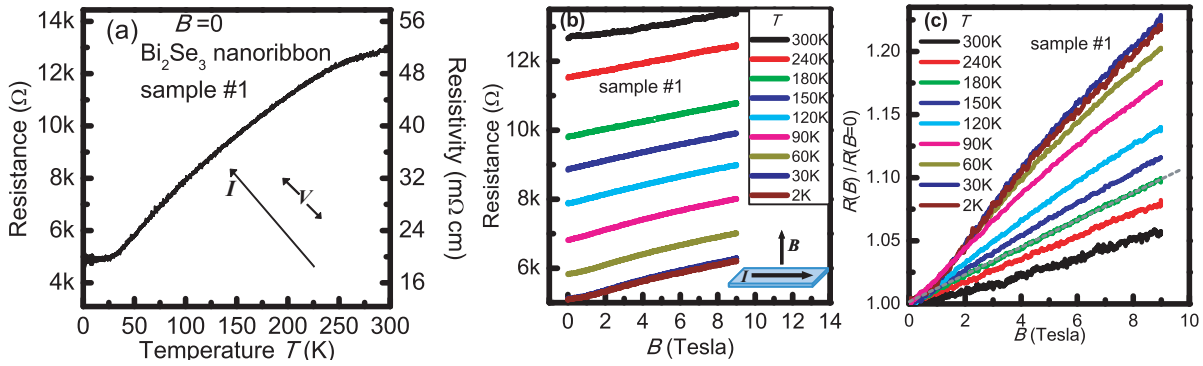

FIG. 1: (color online) (a) Resistance R vs. T of a Bi_2Se_3 nanoribbon (sample #1). The right axis shows resistivity. The inset shows the SEM image of device and illustration of the four-terminal measurement of R. White scale bar is 2μm. (b) R vs. perpendicular magnetic field for sample #1 at various T from 300K to 2K. (c) Data in (b) plotted as $R(B)/R(B=0)$ vs. magnetic field. Above 90K, R varies linearly with B. A grey dashed line is included to guide the eye.

linear and non-saturating at high fields[12]. This is not the case here. The existence of a linear MR for small bandgap semiconductor could have a quantum[10, 13] or classical origin[13, 14]. To explain the linear MR down to very low fields in silver chalcogenides[15], Abrikosov first proposed a model based on the QLMR[16]for systems with gapless linear dispersion spectrum[10]. It is believed that such gapless linear dispersion may apply for silver chalcogenide or other small bandgap semiconductors with strong inhomogeneity[10, 13]. Without invoking the linear dispersion spectrum, Parish and Littlewood suggested a classical origin for linear MR in which the MR is a consequence of mobility fluctuations in a strongly inhomogeneous system[14]. For our Bi_2Se_3 nanoribbons, the single crystal quality and small length scale of the device rule out the models where strong physical inhomogeneity of sample is required. Therefore, it is tempting to attribute the linear MR observed here to the QLMR from Dirac electrons on the Bi_2Se_3 surface, which have very small effective mass and large cyclotron energy[4]. We also point out that Abrikosov's QLMR model predicts a *temperature independent* $\Delta R(B)=R(B)-R(B=0)$[10], which is indeed in agreement with our data in Fig.1b. Therefore, the persistence of linear MR at high T for Bi_2Se_3 nanoribbons is striking: it could indicate the persistence of topological surface-states induced MR up to room temperature.

In an attempt to distinguish the surface electrons from bulk electrons in our Bi_2Se_3 nanoribbons, we performed MR measurements on several samples under various magnetic field orientations. Fig.2a presents the normalized resistance, $R(B)/R(B=0)$, as a function of the perpendicular magnetic field for four nanoribbons. All the data were collected at T=2K except for sample #2 which was measured at 10K. Due to the different carrier density and mobility of these samples, the rate of resistance increase is different. However, we found that all the MR curves collapse onto a single curve if we perform a linear scaling of the magnetic field, as shown in Fig.2b. In Fig.2b, the magnetic field is scaled linearly for sample #1, 2 and 4 against sample #3 which shows the largest MR response. The fact that all the four MR curves can be scaled onto a single curve suggests there is a universal scattering mechanism. Kohler's rule[12] suggests that the MR of a material is a universal function of μB: $R(B)/R(B=0)=F(\mu B)$. It is common[12] that at low field when $\mu B \ll 1$, $F(\mu B)\approx 1+(\mu B)^2$, as a result of the Lorentz force deflection of carriers, with μ as the carrier mobility. As shown in Fig2.b, our low T MR data are in good agreement with Kohler's rule and exhibit a B^2 dependence at low B. Using Kohler's rule, one can estimate the mobility μ from the parabolic MR at low B[17]. We estimate that $\mu\approx$1000, 525, 1500, and 750 $cm^2/V\cdot s$ for our nanoribbon sample 1, 2, 3 and 4 at lowest T. These mobility values are somewhat lower than values previously reported on Bi_2Se_3 nanoribbons[8, 9] and are about 10 times lower than high quality bulk single crystals[18–21]. According to conventional MR theory of metals, MR$\propto(\mu B)^2$ and saturates at high field ($\mu B>1$). However, our samples did not show saturation of MR at high B. Instead, the MR shows a crossover from B^2 to linear B dependence (Fig.2b). Based on the estimated value of μ, we can see that the crossover from B^2 to linear B dependence in our MR data in Fig.2 indeed happens at μB$\sim$1. The high field behavior of MR$\propto B$ in Fig.2 is reminiscent of Abrikosov's QLMR[10], which occurs at $\hbar\omega_c > E_F$, when all electrons coalesce into the lowest Landau level. Here $\hbar$ is the reduced Planck's constant, $\omega_c=eB/m^*$ is the cyclotron frequency with m^* being the electron effective mass, e being the electron charge and E_F being the Fermi energy. Using our estimates of Fermi momentum and electron concentration(10^{17}-$10^{18}/cm^3$) described later in the paper, the emerging of QLMR at B >$\sim$5T in Fig.1 would correspond to around 3 Lan-

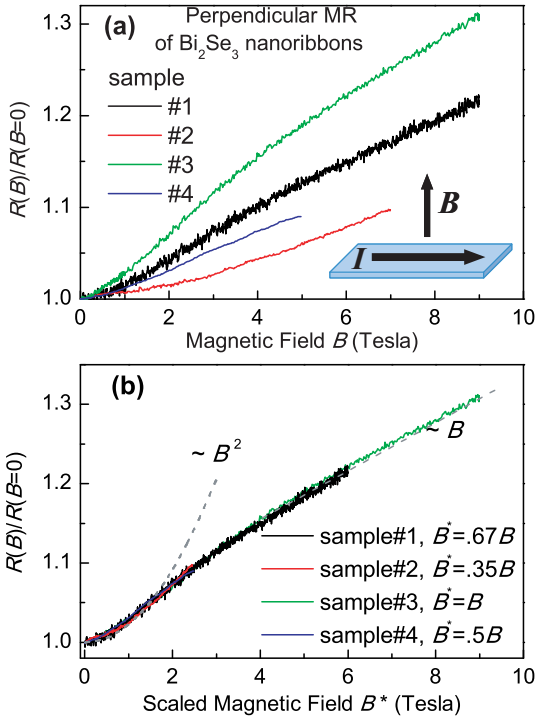

FIG. 2: (color online) (a) The normalized resistance $R(B)/R(B{=}0)$ vs. perpendicular B for four Bi_2Se_3 nanoribbons. Except for sample #2 where T=10K, all the data are collected at 2K. (b) $R(B)/R(B{=}0)$ vs. scaled magnetic field B^* for samples in (a). The magnetic field is scaled linearly for sample #1, 2 and 4 against #3 which shows the largest MR response. Consistent with the Kohler's rule, all MR curves collapse onto a single curve after scaling. MR has a B^2 dependence at low field and linear B dependence at high field as shown by the grey dashed lines.

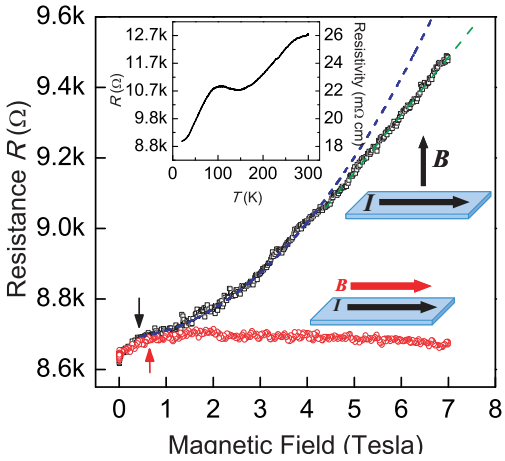

FIG. 3: (color online) The perpendicular MR compared with the longitudinal MR at T=10K for Bi_2Se_3 nanoribbon sample #2. The blue dashed line shows the B^2 dependence of MR below 4Telsa. The black and red arrows mark the initial rise of the MR which is attributed to boundary-scattering effect. The inset shows the resistance and resistivity vs T data at B=0.

dau levels being filled. It is worth to note that our low T(<90K) MR data and analysis are in qualitative agreement with bulk InSb where the QLMR is also found to emerge at high filling factors[13]. With this understanding of MR at low T, it is enlightening to re-examine the overall evolution of $R(B)$ from 2K to 300K in Fig.1b. It is clear that as T rises, the high field linear B behavior persists into lower field, suggesting that the QLMR is actually more significant at high temperatures. Since most likely bulk electrons coexist with surface electrons in the sample, the disappearance of quadratic MR at high temperature is possibly related to the different contributions from bulk and surface states at different T.

Now let us turn to the comparison of MR between different field orientations. Zero field R vs T of nanoribbon sample #2 is shown in Fig.3 inset. The peak around T=100K in the $R(T)$ curve for this sample resembles those of low doped Bi_2Se_3 bulk samples[18]. Assuming homogeneous conduction through the sample, the 3D resistivity is shown on the right axis of Fig.3 inset using the size of this nanoribbon measured by atomic force microscopy (AFM) (length L=2.34μm, width W=600nm and thickness H=80nm). Fig.3 main panel compares the 10K MR of sample #2 in perpendicular vs. longitudinal magnetic fields. The perpendicular MR exhibits a quadratic behavior below 4T and is much larger than the longitudinal one. It can be noticed that for both field orientations, there is an initial step-like rise of MR at low B (<1T) as marked by the black and red arrows. This feature is more salient in samples with lower noise (e.g. sample #3 in Fig.4 below) and only observed at low T (10K or lower). We attribute this step-like rise of MR at the lowest B to the boundary scattering of electrons undergoing cyclotron motion in our nanoribbons with finite size. A similar effect was observed for electrons in Bi and Sb nanowires[22, 23] as well as 2D electrons in GaAs heterostructure samples with narrow width[24]. Briefly, due to the finite size of sample, the bending of electrons' trajectories by the Lorentz force enhances the surface scattering when B increases from zero, and such surface scattering leads to the rise of sample resistance. However, as B increases to a critical field B_c, where the size of the cyclotron orbital is comparable with the size of sample, the increase of surface scattering rate slows down and therefore the resistance rise stops. At $B > B_c$, we do not detect any features like the A-B oscillations in the longitudinal MR, presumably due to the lower mobility and shorter coherence length of our sample than those in Ref.[8].

We also compared the perpendicular vs transverse (B parallel to sample surface but transverse to current) magneto-transport of Bi_2Se_3 nanoribbon sample #3. Our experiment shows that the transverse MR is also negligible except for the initial step-like increase of

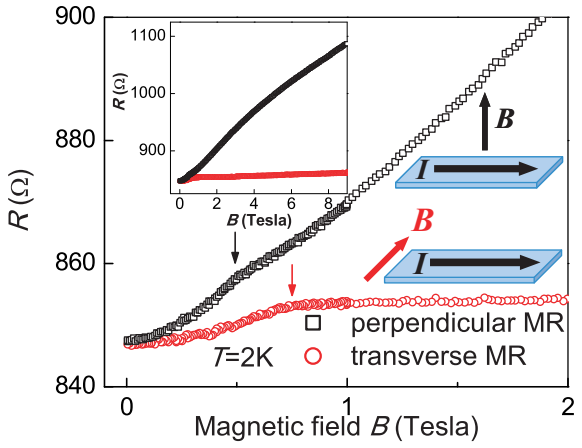

FIG. 4: (color online) Perpendicular (black squares) vs transverse (red dots) MR of Bi_2Se_3 nanoribbon sample #3 at T=2K. The nanoribbon is 900nm wide and 160nm thick. The black/red arrow highlights the critical magnetic field B_c for the boundary-scattering (see text). The inset shows the data on a larger scale (B=0-9Tesla).

MR at low B, in a similar way to longitudinal MR, as shown in Fig.4a and the inset. Due to the low noise of sample #3, the finite-size-induced boundary scattering effect in the low B regime of MR can be clearly resolved, with B_c∼0.5T for perpendicular field and B_c∼0.75T for transverse field. The critical field B_c corresponds to the condition $r_c = d/2$ where $r_c = \hbar k_F/eB_c$ is the cyclotron radius and d is the smallest dimension of the sample in the plane of cyclotron motion[22–25]. Since both the length, width and thickness of our nanoribbons are known (measured by AFM), we can use the critical field B_c and criterion $r_c = \hbar k_F/eB_c = d/2$ to estimate k_F , the Fermi momentum, as suggested first by Chambers[25]. For the perpendicular field case, the relevant d is the sample width W, and we estimate a $k_F \sim WeB_c/2\hbar = 3.6\times10^8 \mathrm{m}^{-1}$ using W=900nm and B_c∼0.5T. For the transverse field configuration, the relevant d is the sample thickness H, and we estimate a $k_F \sim HeB_c/2\hbar = 1\times10^8 \mathrm{m}^{-1}$ using H=160nm and B_c∼0.75T. Note that k_F extracted in the perpendicular field configuration is always a few times larger than the transverse or longitudinal case for our nanoribbons. This difference is at odds with the Fermi surface topology of bulk Bi_2Se_3 probed by Shubnikov de-Haas effect[20], which shows that k_F along c-axis (perpendicular to nanoribbon surface) should be slighter larger than the in-plane k_F if bulk electrons are involved. Since the k_F estimated from the boundary scattering effect is an averaged k_F over the cyclotron orbit in the plane perpendicular to B, this discrepancy suggests that k_F perpendicular to nanoribbon surface is very small and is likely due to the confinement effect and/or more dominant contribution from the surface states in nanoribbon samples. Nevertheless, the magnitude of k_F is comparable with a 3D electron concentration on the order of 10^{17}- $10^{18}/\mathrm{cm}^3$[20] or a 2D electron concentration on the order of $10^{12}/\mathrm{cm}^2$. To make the quasi-2D surface states dominate over bulk states, it is expected the carrier concentration should be low. Thus the relatively low carrier concentration inferred here is reasonable.

Finally, we make a few comments on separating the the surface states from bulk electrons in the MR effects. While all the existing data in literature suggest that both the bulk and surface electrons contribute to the electrical transport, the linear MR we observed at high T is quite consistent with the topological surface states with linear dispersion and hard to explain in conventional theory without introducing strong sample inhomogeneity. Although the boundary-scattering-induced MR effect at low field has been discussed in a 3D picture for Bi and Sb nanowires[22, 23], it does not exclude the possibility of being originated from surface electrons. What is more important is that our study of MR in different field orientations reveals that k_F perpendicular to nanoribbon surface is much smaller than k_F in the plane. This contradicts the simple 3D Fermi surface picture[20] but is more consistent with having an origin from quasi-2D surface electrons. All this suggests that the MR effects observed are non-trivial and may have connection with topological surface states with linear dispersion spectrum.

In summary, we report MR of chemically synthesized Bi_2Se_3 nanoribbons under various magnetic field orientations. When the magnetic field is parallel to the surface of nanoribbon (a-b plane), the MR effect is much smaller than in a perpendicular field. At the lowest B(<1T), we observe boundary scattering induced MR, from which it is concluded that k_F perpendicular to surface is much smaller than k_F in the plane. As B increases such that boundary scattering is unimportant, the low T perpendicular MR exhibits a B^2 dependence which crosses over to a non-saturating linear behavior at high field. This linear MR extends to zero field as T raises. The linear MR is attributed to Abrikosov's QLMR and seems to be consistent with the existence of electrons having linear dispersion spectrum, as predicted in the topological insulator theory.

X.P.A. Gao acknowledges P.B. Littlewood for discussion, ACS Petroleum Research Fund (grant 48800-DNI10) and NSF (grant DMR-0906415) for financial support.

* xuan.gao@case.edu

[1] S.C. Zhang, Physics **1**, 6 (2008).
[2] J.E. Moore, Nature **464**, 194 (1958).
[3] M.Z. Hasan, C.L.Kane, arXiv:1002.3895v1.
[4] H.J. Zhang, *et al*, Nature Phys. **5**, 438 (2009).
[5] D. Hsieh,*et al*,Nature **452**, 970 (2008).
[6] Y. Xia, *et al*, Nature Phys. **5**, 398 (2009).
[7] D. Hsieh,*et al*, Nature **460**, 1101 (2009).

[8] H.L. Peng, *et al*, Nature Mat. **9**, 225 (2010).
[9] D. Kong, *et al*, Nano Lett. **10**, 329 (2010).
[10] A.A. Abrikosov, Phys. Rev. B **58**, 2788 (1998).
[11] Tuning sample resistance by a backgate shows n-type behavior for all our samples, indicating electron as the majority carrier.
[12] J.L. Olsen, Electron Transport in Metals, Interscience, New York, (1962).
[13] J.S. Hu, T.F. Rosenbaum, Nature Mat. **7**, 697 (2008).
[14] M.M. Parish, P.B. Littlewood, Nature **426**, 162 (2003).
[15] R. Xu, *et al*, Nature **390**, 57 (1997).
[16] A.A. Abrikosov, Europhys. Lett. **109**,49,789 (2000).
[17] G.R. Hyde, H.A. Beale, I.L. Spain, J.A. Woollam, J. Phys. Chem. Solids **35**, 1719 (1974).
[18] J.G. Checkelsky,*et al.*, Phys. Rev. Lett. **103**, 246601 (2009).
[19] J.G. Analytis, *et al.*, arXiv:1001.4050.
[20] K. Eto, *et al.*, arXiv:1001:5353.
[21] N.P. Butch, it et al., arXiv:1003.2382.
[22] J. Heremans, *et al.*, Phys. Rev. B **61**, 2921 (2000).
[23] J. Heremans, C.M. Thrush, Y.M. Lin, S.B. Cronin, M.S. Dresselhaus, Phys. Rev. B **63**, 085406 (2001).
[24] T.J. Thornton, M.L. Roukes, A. Scherer, B.P. Van de Gaag, Phys. Rev. Lett. **63**, 2128 (1989).
[25] R.G. Chambers, Proc. R. Soc. London, Ser.A. **202**, 378 (1950).